BT 601: Analytical Biotechnology

-Prof. Siddhartha Sankar Ghosh

Lec-17

Application of Spectrophotometry in Centrifugation

What is Centrifugation?

Centrifugation is a way to increase the magnitude of the gravitational field so that particles in suspension experience a radial centrifugal force that moves them away from the axis of rotation.

Sedimentation:

1. Density
2. Under Gravity

Interpretation of sedimentation velocity

"How fast does an object sediment under normalized conditions?"

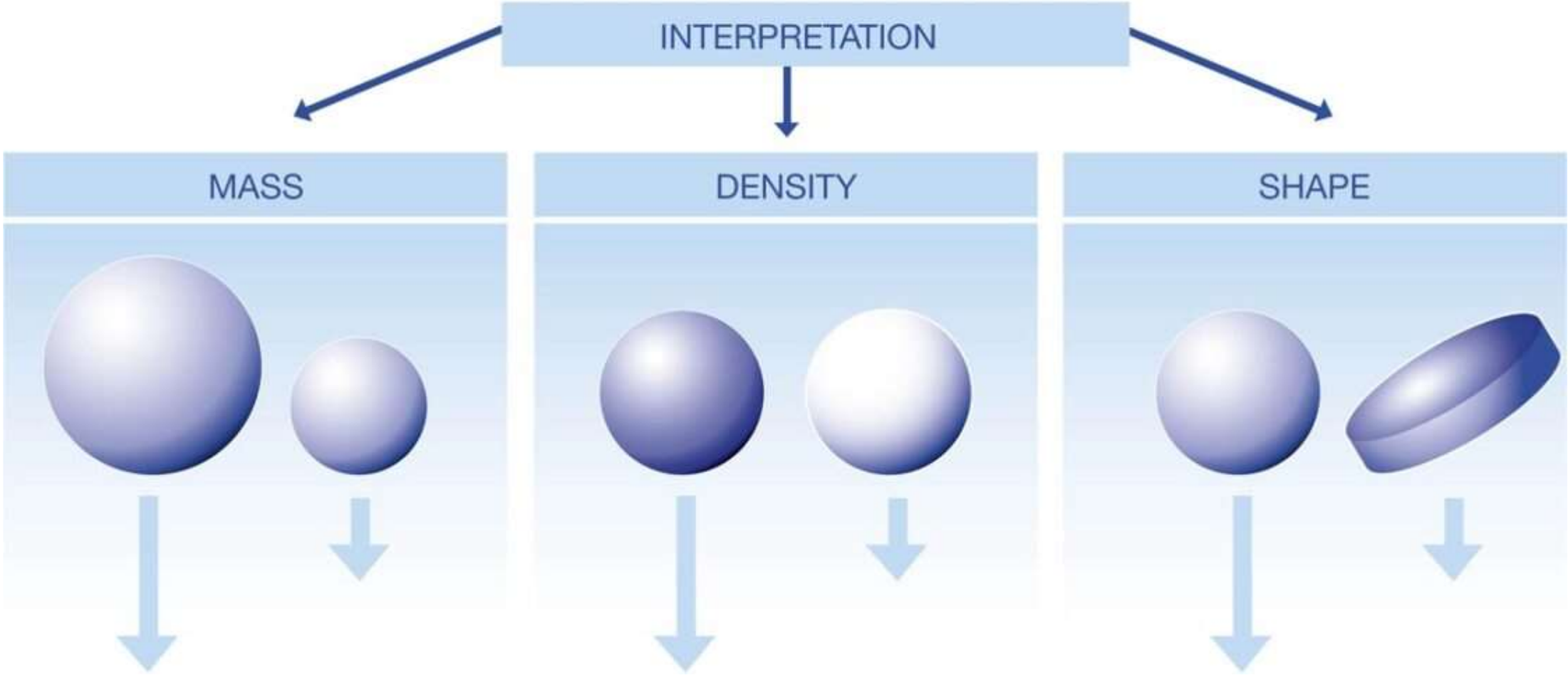

Basics of Centrifuge

Working Principle:

- A centrifuge works by using the principle of sedimentation, that is, separating substances according to density, under the influence of gravity.
- Separation may be of many varieties, like ultrafiltration, phase separation, density gradient, and pelleting.
- Pelleting is the most commonly used procedure. It refers to the concentration of particles in a pellet, at the bottom of the centrifuge, thus separating it from the solution remaining, also known as the supernatant.
- The relative centrifugal force (rcf) and the degree of acceleration in multiples of acceleration due to gravity(g) are typically specified, since the concept of using rotational speed, like revolutions per minute (rpm), is quite imprecise.

Basics of Centrifuge

What is Relative Centrifugal Force?

The relative centrifugal force (RCF) or the g force is the radial force generated by the spinning rotor as expressed relative to the earth's gravitational force. The g force acting on particles is exponential to the speed of rotation defined as revolutions per minute (RPM).

Doubling the speed of rotation increases the centrifugal force by a factor of four. The centrifugal force also increases with the distance from the axis of rotation. These two parameters are of considerable significance when selecting the appropriate centrifuge.

RPM and RCF

1.RPM: The particles travel radially away about the rotation axis with the help of the centrifugal force, while the suspension rotates at a specified speed or **revolutions per minute (RPM**). The revolutions per minute of a centrifuge are calculated using the following formula:

$$RPM = \sqrt{\frac{g}{r}},$$

g = respective force of the centrifuge, r = radius from the center of the rotor to a point in the sample.

2. **Relative Centrifugal Force (RCF)** usually refers to the particle force in comparison to the gravitational force. This force relative to gravity is exerted on the materials within the rotor, perpendicular to the surface, in response to the rotation, measuring rotors of different types and sizes. For example, an RCF of 1000 x g implies the gravitational force of the earth is 1000 times weaker than the centrifugal force. It depends on the speed of rotation in rpm and the distance of the particles about the center of rotation.

Formulation:

- Since the particles are being separated by gravitational force, the rate of separation varies according to the particle size and density.
- Particles of higher density or size are separated from particles with less density or size, at a certain point, since they travel at a faster rate.
- Stoke's law, a law that describes the movement of a sphere under the influence of gravity, is used to explain the sedimentation of particles.

The force of viscosity on a small sphere moving through a viscous fluid is given by:

$$F = 6\pi r\eta v$$

Ultracentrifuge

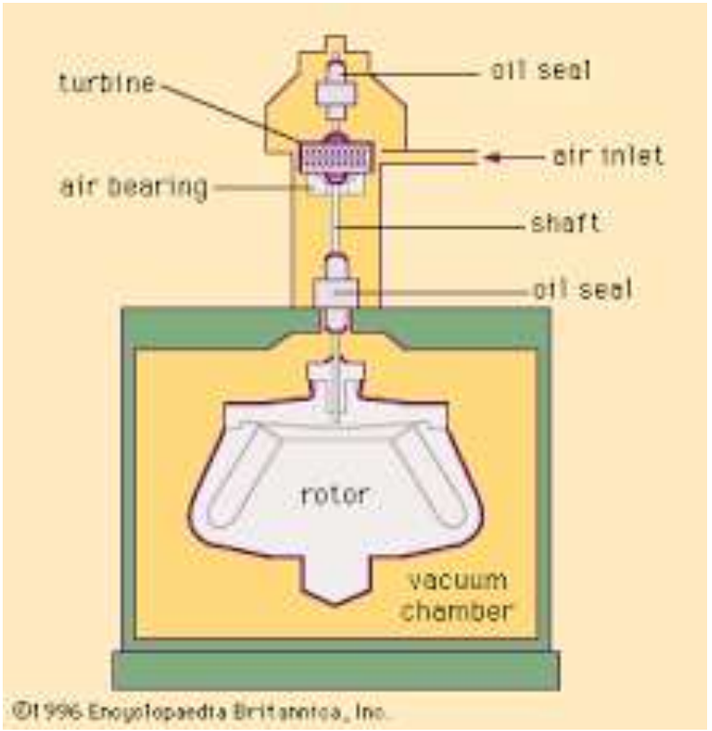

The ultracentrifuge is a centrifuge optimized for spinning a rotor at very high speeds, capable of generating acceleration as high as 1 000 000 g (approx. 9 800 km/s²).

Analytical Ultracentrifuge

- **Analytical ultracentrifugation** is an analytical technique which combines an ultracentrifuge with optical monitoring systems.
- In an analytical ultracentrifuge (commonly abbreviated as AUC), a sample's sedimentation profile is monitored in real time by an optical detection system.
- The sample is detected via ultraviolet light absorption and/or interference optical refractive index sensitive system, monitored by light-sensitive diode array.
- The change of sample concentration versus the axis of the rotation profile with time as a result of the applied centrifugal field can be observed.
- Most common AUC experiments are sedimentation velocity and sedimentation equilibrium experiments.

Analytical Ultracentrifuge: Animation Video

The following features make Analytical Ultracentrifugation such a valuable tool in colloid and biophysical analysis:

- ❑ Analytical Ultracentrifugation is an absolute method.
- ❑ Analytical Ultracentrifugation is a dispersive method; mixtures are fractionated during analysis.
- ❑ Analytical Ultracentrifugation gives access to geometric (size, shape, structure) and thermodynamic properties (equilibrium constants, free energies, enthalpies, entropies).
- ❑ With a maximum angular velocity of 60,000 rpm, equivalent to Earth's gravity 260,000-fold, Analytical Ultracentrifugation is applicable for a particle size range from 1 to 1000 nm and a molecular mass range from ca. 2,000 Da to hundreds of MDa.
- ❑ Arbitrary solvents can be applied.
- ❑ A wide range of concentrations is accessible – formulations can be examined in their original state (depending on suitable instrumentation)
- ❑ Detection is most versatile due to multiple, synchronous optical systems.
- ❑ Complex mixtures are fractionated with high statistical reliability, as all sedimenting objects are detected.
- ❑ Combination of sedimentation and spectroscopic properties allows characterization by orthogonal information.

Analytical Ultracentrifuge

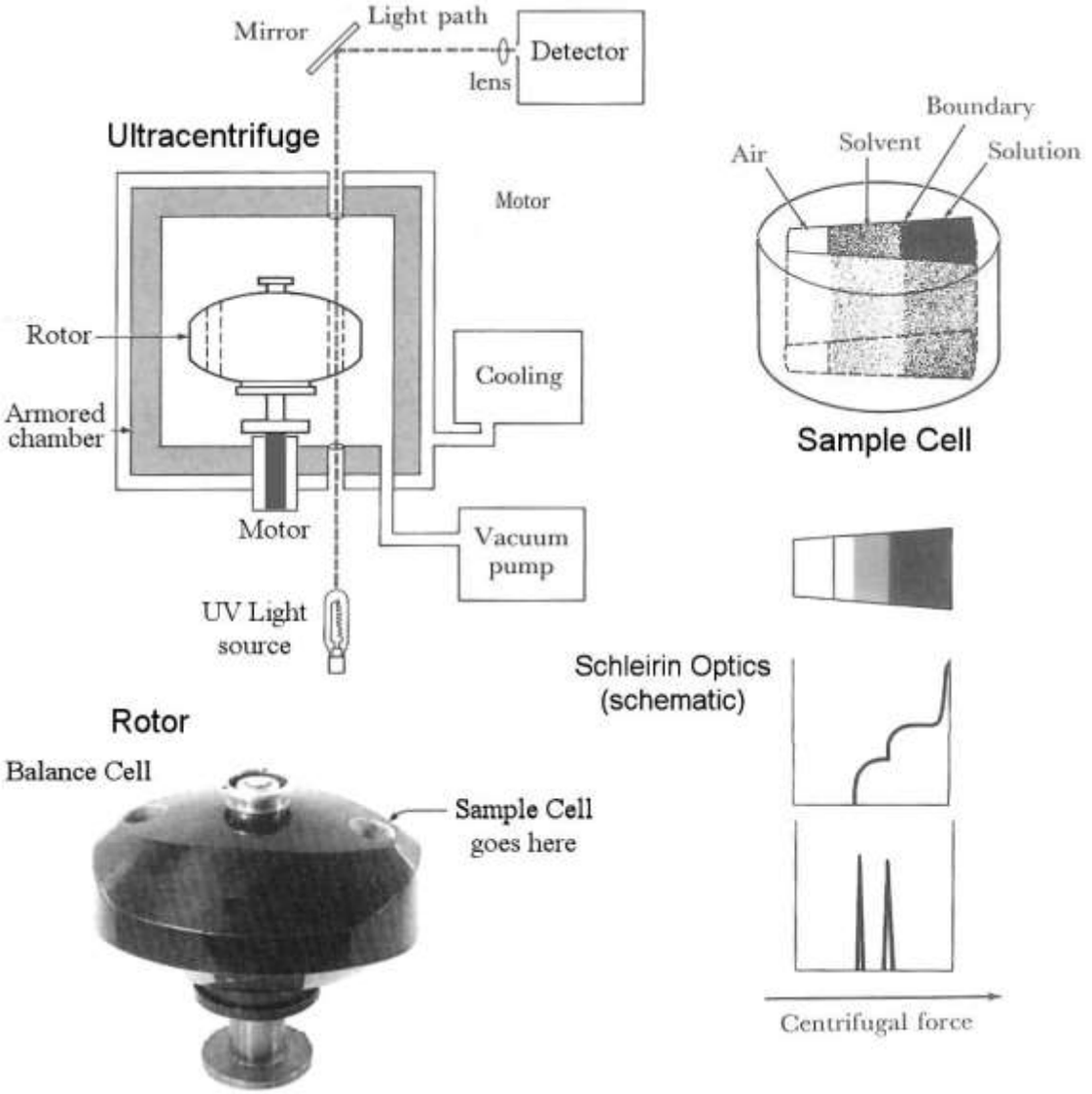

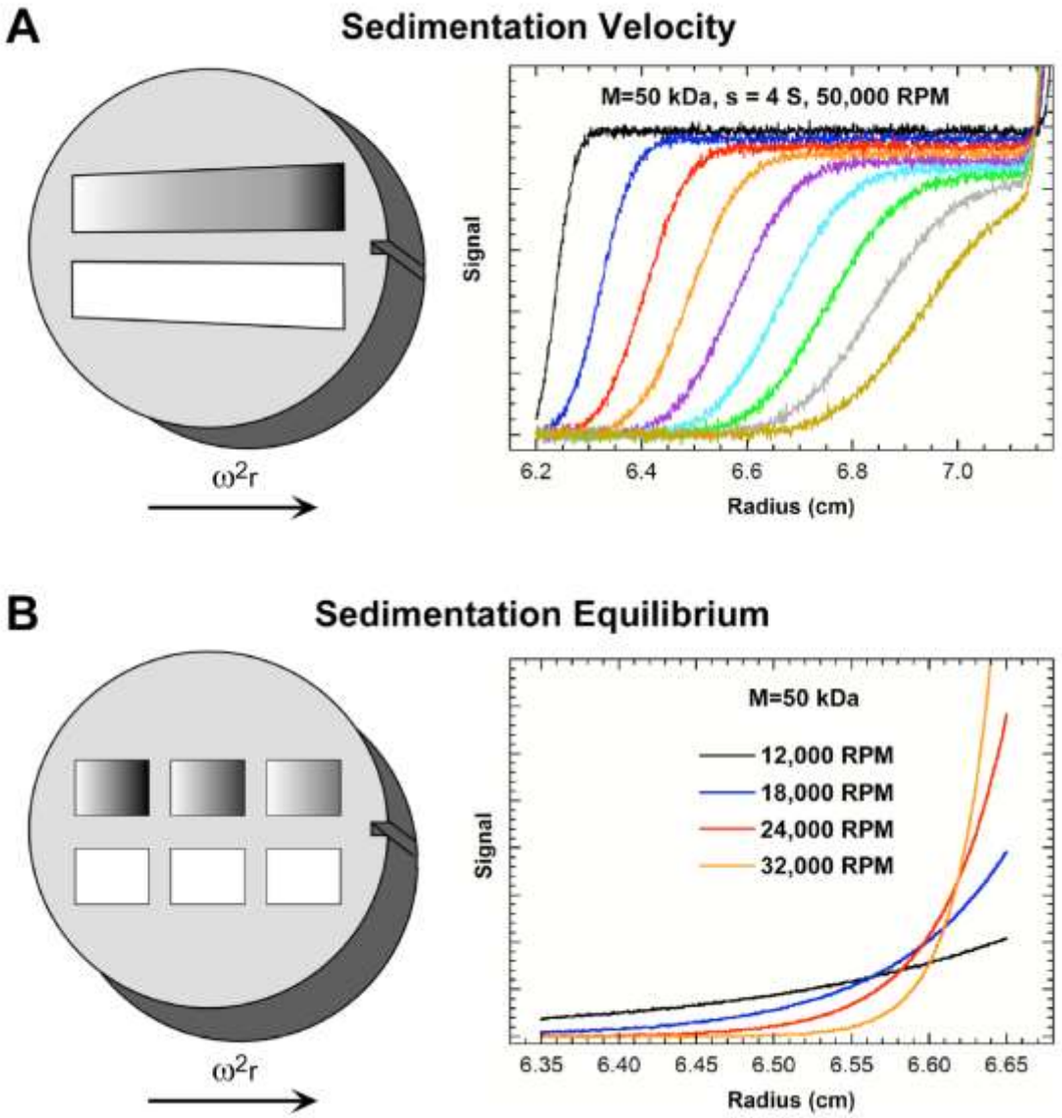

Basic analytical ultracentrifugation experiments. Simulations are for a protein of **50 kDa** with a sedimentation coefficient of 4 S.

A) SV experiment. Velocity sedimentation is usually performed using a two-sector cell and scans are recorded at fixed intervals during the run. The simulation is for a rotor speed of 50,000 RPM and scans are displayed at 20 minute intervals.

B) SE experiment. Equilibrium measurements usually employ a six sector cell with three loading concentrations. The equilibrium concentration gradients are simulated for rotor speeds ranging between 12,000–32,000 RPM, corresponding to values of ranging from ~ 0.8 to ~ 6 cm^{-2}.

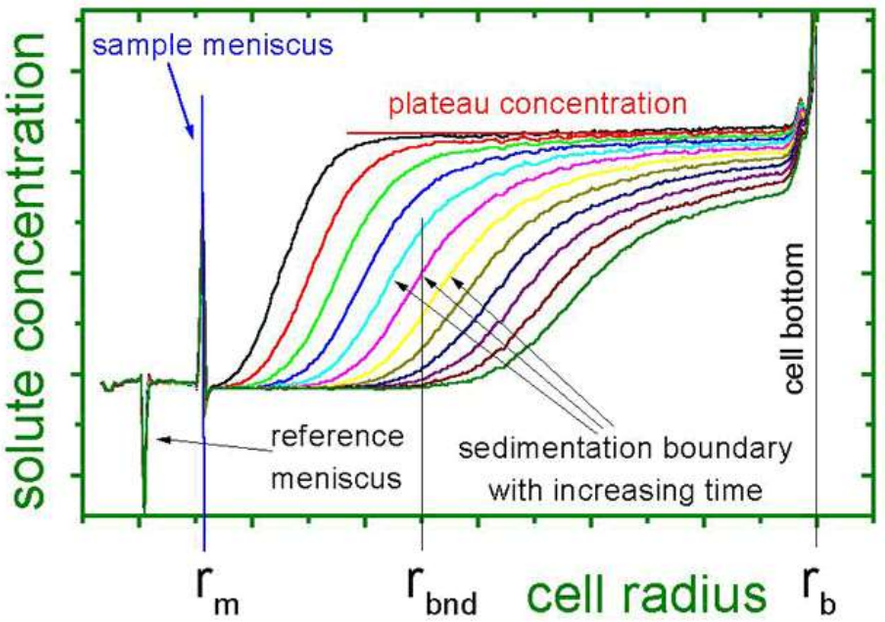
sample meniscus
plateau concentration
solute concentration
cell bottom
reference
meniscus
sedimentation boundary
with increasing time
r m
r bnd
cell radius
r b

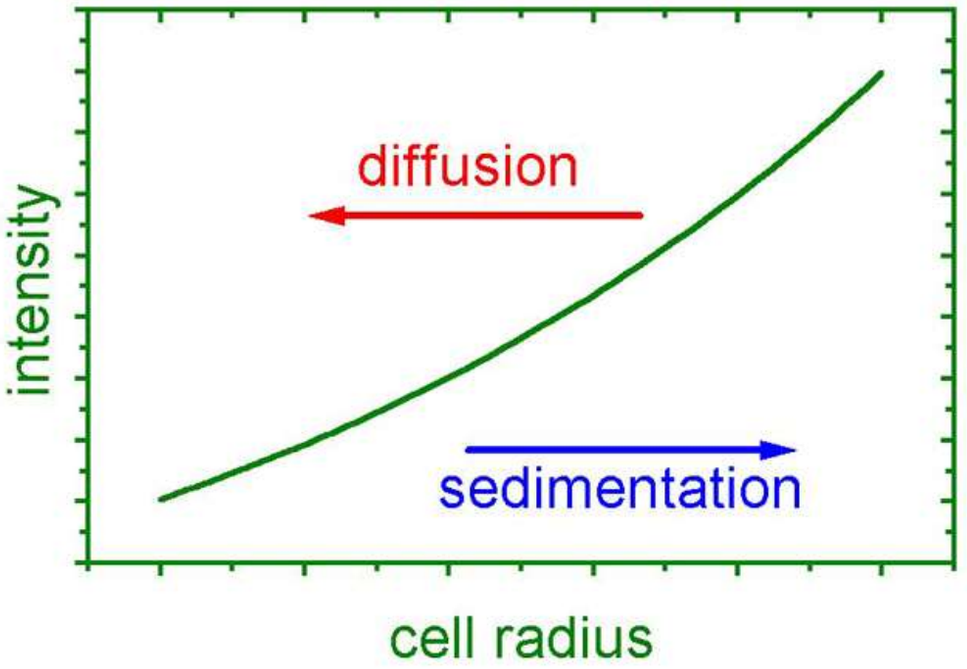
diffusion
intensity
sedimentation
cell radius

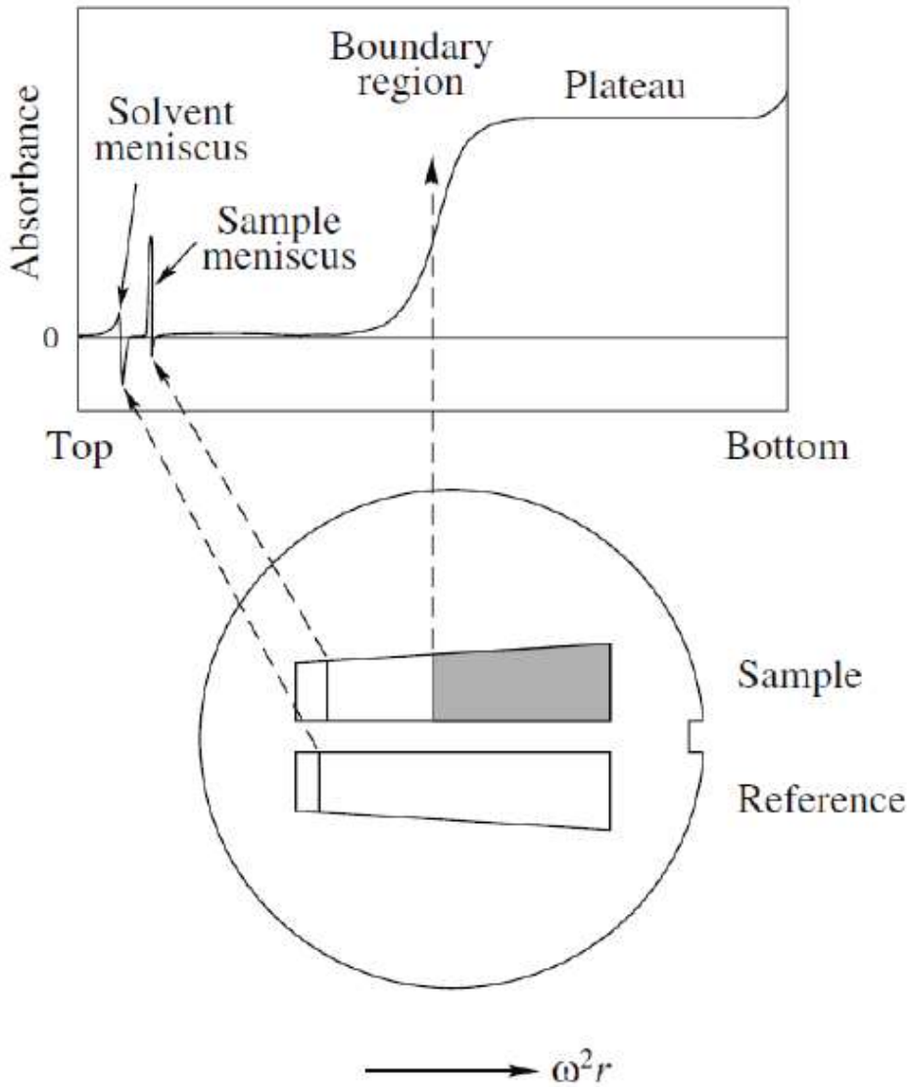

Figure 2. Double-sector centerpiece. The sample solution is placed in one sector, and a sample of the solvent in dialysis equilibrium with the sample is placed in the reference sector. The reference sector is usually filled slightly more than the sample sector, so that the reference meniscus does not obscure the sample profile.

SEDIMENTATION OF PARTICLES IN A GRAVITATIONAL FIELD: Governing equations

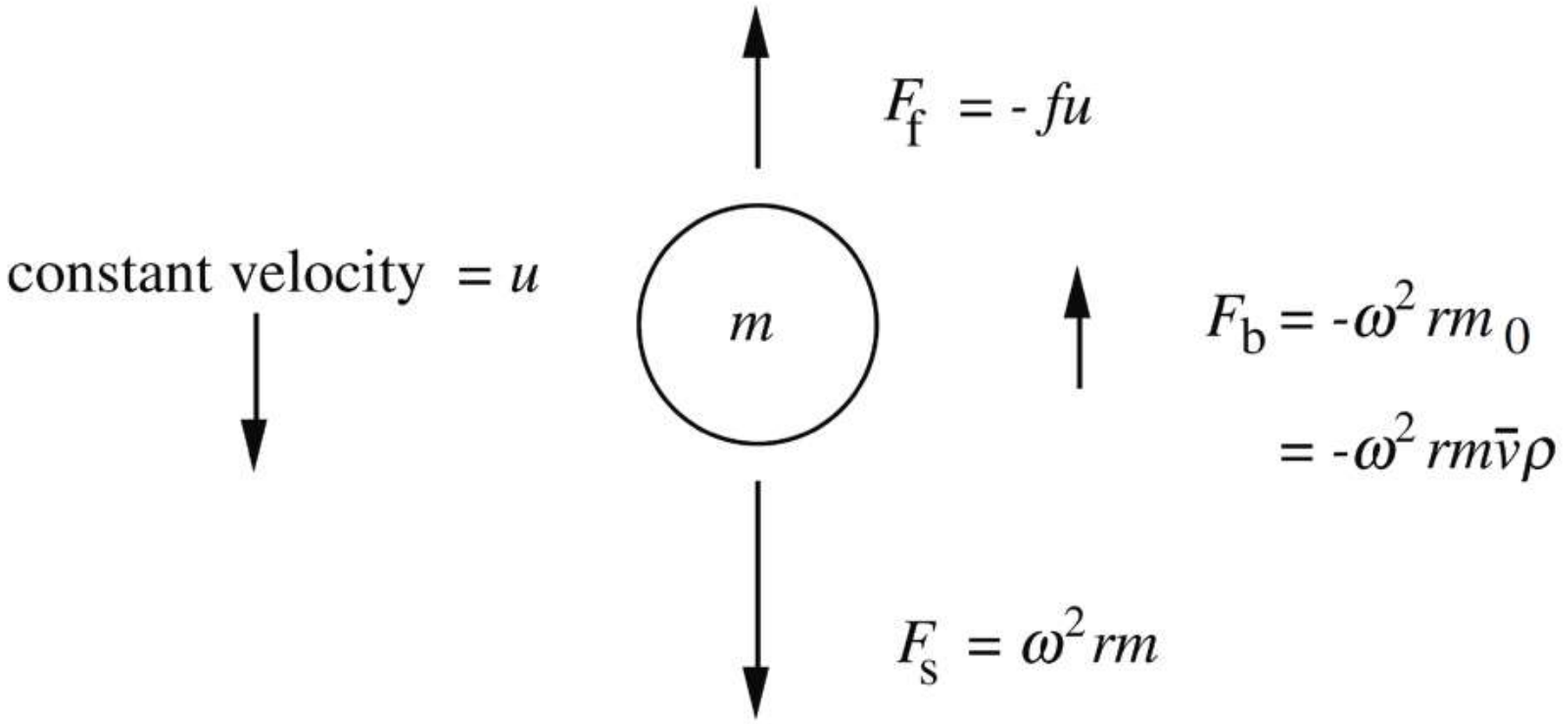

Figure 1. The forces acting on a solute particle in a gravitational field

First, there is a sedimenting, or gravitational force, F_s, proportional to the mass of the particle and the acceleration. In a spinning rotor, the acceleration is determined by the distance of the particle from the axis of rotation, r, and the square of the angular velocity, ω (in radians per second).

1

$$F_s = m\omega^2 r = \frac{M}{N}\omega^2 r$$

where m is the mass in grams of a single particle, M is the molar weight of the solute in g/mol and N is Avogadro's number. (Note that the molecular weight is numerically equal to the molar weight, but is dimensionless.)

Second, there is a buoyant force, F_b, that, from Archimedes' principle, is equal to the weight of fluid displaced:

2 $$F_b = -m_0\omega^2 r$$

where m_0 is the mass of fluid displaced by the particle:

3 $$m_0 = m\bar{v}\rho = \frac{M}{N}\bar{v}\rho$$

Here, $\bar{v}$ is the volume in mL that each gram of the solute occupies in solution (the partial specific volume; the inverse of its effective density) and ρ is the density of the solvent (g/mL). Provided that the density of the particle is greater than that of the solvent, the particle will begin to sediment.

4 $$F_f = -fu$$

where f is the frictional coefficient, which depends on the shape and size of the particle. Bulky or elongated particles experience more frictional drag than compact, smooth spherical ones. The negative signs in equations (2) and (4) indicate that these two forces act in the opposite direction to sedimentation.

Within a very short time (usually less than 10^{-6} s) the three forces come into balance:

5 $$F_s + F_b + F_f = 0$$

6 $$\frac{M}{N}\omega^2 r - \frac{M}{N}\bar{v}\rho\omega^2 r - fu = 0$$

Rearranging:

7 $$\frac{M}{N}(1 - \bar{v}\rho)\omega^2 r - fu = 0$$

Collecting the terms that relate to the particle on one side, and those terms that relate to the experimental conditions on the other, we can write:

8

$$\frac{M(1 - \bar{v}\rho)}{Nf} = \frac{u}{\omega^2 r} \equiv s$$

- The term $u/\omega^2 r$, the velocity of the particle per unit gravitational acceleration, is called the sedimentation coefficient, and can be seen to depend on the properties of the particle.
- It is proportional to the buoyant effective molar weight of the particle (the molar weight corrected for the effects of buoyancy) and it is inversely proportional to the frictional coefficient.
- Molecules with different molecular weights, or different shapes and sizes, will, in general, move with different velocities in a given centrifugal field; i.e., they will have different sedimentation coefficients. The sedimentation coefficient has dimensions of seconds. For many substances, the value of s lies between 1 and 100 × 10-13 seconds.
- The **Svedberg unit** (abbreviation S) is defined as 10-13 seconds, in honor of Thé Svedberg.

SEDIMENTATION OF PARTICLES IN A GRAVITATIONAL FIELD: Governing equations

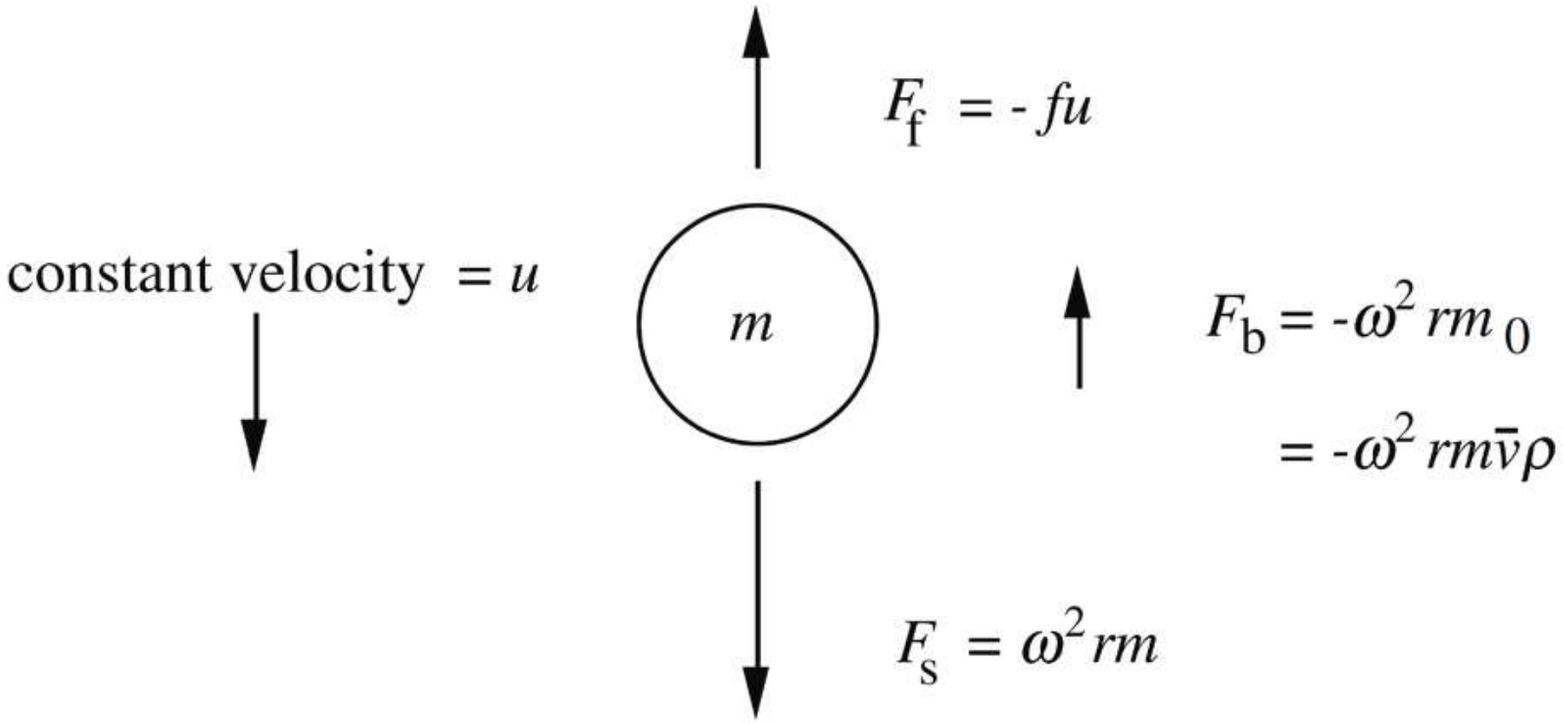

Figure 1. The forces acting on a solute particle in a gravitational field

Collecting the terms that relate to the particle on one side, and those terms that relate to the experimental conditions on the other, we can write:

8

$$\frac{M(1 - \bar{v}\rho)}{Nf} = \frac{u}{\omega^2 r} \equiv s$$

- The term $u/\omega^2 r$, the velocity of the particle per unit gravitational acceleration, is called the sedimentation coefficient, and can be seen to depend on the properties of the particle.
- It is proportional to the buoyant effective molar weight of the particle (the molar weight corrected for the effects of buoyancy) and it is inversely proportional to the frictional coefficient.
- Molecules with different molecular weights, or different shapes and sizes, will, in general, move with different velocities in a given centrifugal field; i.e., they will have different sedimentation coefficients. The sedimentation coefficient has dimensions of seconds. For many substances, the value of s lies between 1 and 100 × 10-13 seconds.
- The **Svedberg unit** (abbreviation S) is defined as 10-13 seconds, in honor of Thé Svedberg.

Measurement of the rate of spreading of a boundary can lead to a determination of the *diffusion coefficient*, D, which depends on the effective size of the particles:

10 $$D = \frac{RT}{Nf}$$

where R is the gas constant and T the absolute temperature. The ratio of the sedimentation to diffusion coefficient gives the molecular weight:

11 $$M = \frac{s^0 RT}{D^0(1 - \bar{v}\rho)}$$

where M is the molar weight of the solute, $\bar{v}$ its partial specific volume, and ρ is the solvent density. The superscript zero indicates that the values of s and D, measured at several different concentrations, have been extrapolated to zero concentration to remove the effects of interactions between particles on their movement

DETERMINATION OF *s*

Provided that the sedimenting boundary is relatively sharp and symmetrical, the rate of movement of solute molecules in the plateau region can be closely approximated by the rate of movement of the midpoint, r_{bnd}. This point, in turn, is very close to the position of the point of inflection (which is the same as the maximum ordinate, or "peak," of the *dc/dr* curve).

Since the sedimenting force is not constant, but increases with *r*, the velocity of the boundary will increase gradually with movement of the boundary outwards, so the velocity must be expressed as a differential:

12 $$s \equiv \frac{u}{\omega^2 r} = \frac{dr_{bnd}/dt}{\omega^2 r}$$

Whence:

13 $$\ln(r_{bnd}/r_m) = s\omega^2 t$$

where r_m is the radial position of the meniscus.

SEDIMENTATION VELOCITY

There are two basic types of experiment with the analytical ultracentrifuge: **sedimentation velocity** and **sedimentation equilibrium**

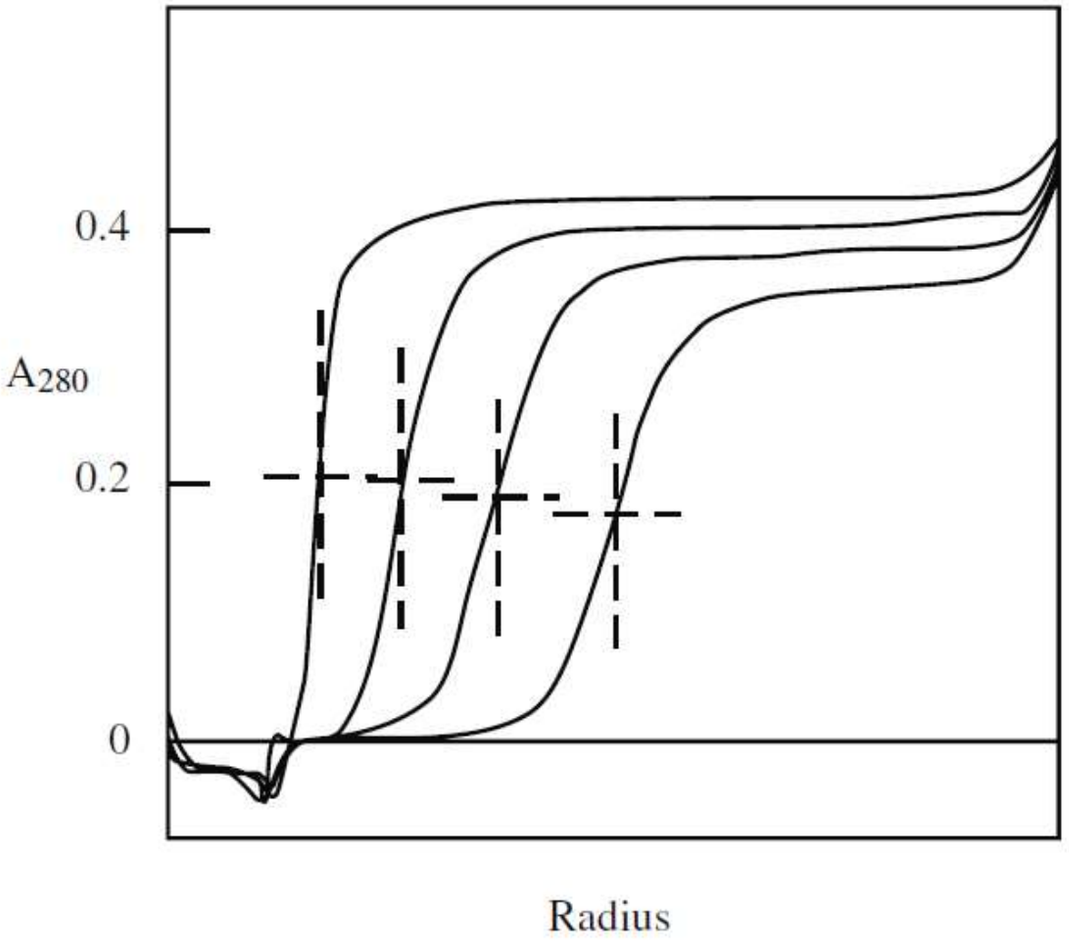

Figure 5. Movement of the boundary in a sedimentation velocity experiment with a recombinant malaria antigen protein. As the boundary progresses down the cell, the concentration in the plateau region decreases from radial dilution, and the boundary broadens from diffusion. The midpoint positions, rbnd, of the boundaries are indicated.

Key Points

- In sedimentation velocity experiment, an initially uniform solution is placed in the cell and a sufficiently high angular velocity is used to cause relatively rapid sedimentation of solute towards the cell bottom.
- This produces a depletion of solute near the meniscus and the formation of a sharp boundary between the depleted region and the uniform concentration of sedimenting solute (the plateau)
- Although the velocity of individual particles cannot be resolved, the rate of movement of this boundary can be measured.
- This leads to the determination of the sedimentation coefficient, s, which depends directly on the mass of the particles and inversely on the frictional coefficient, which is in turn a measure of effective size.

A plot of lnrbnd versus time in seconds yields a straight line of slope sω2.

The slope of this plot yields the **sedimentation coefficient**

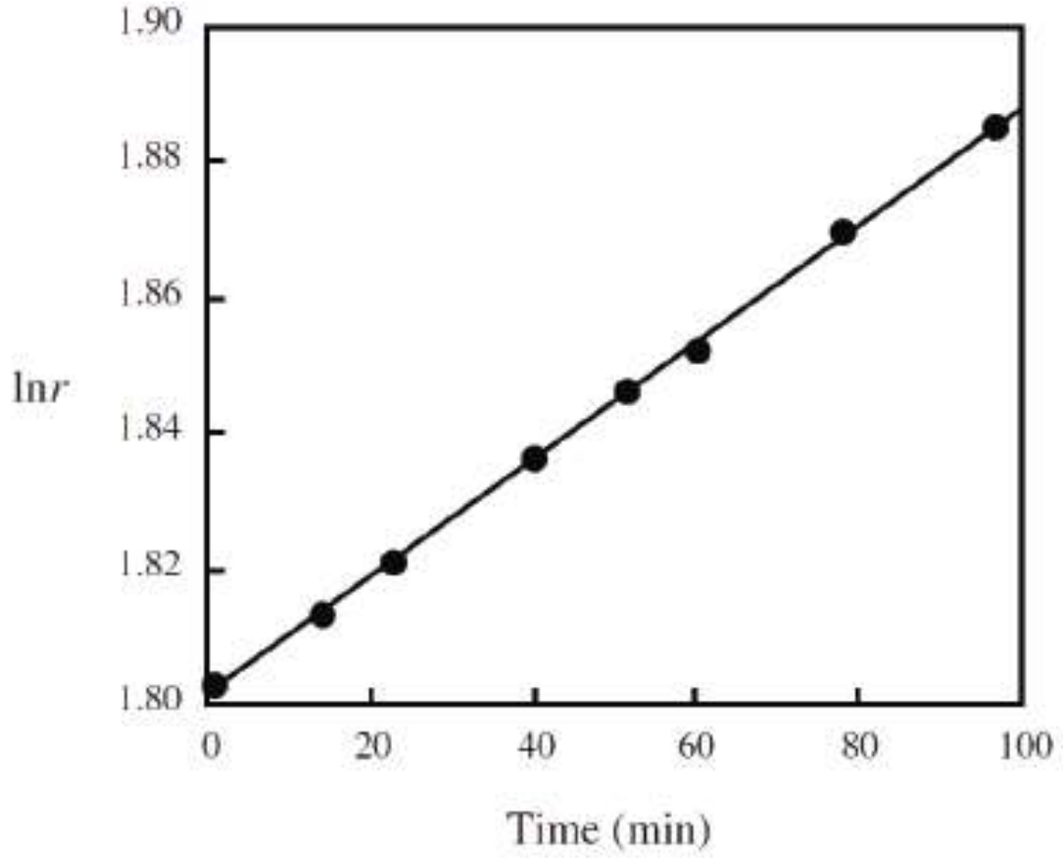

SEDIMENTATION EQUILIBRIUM

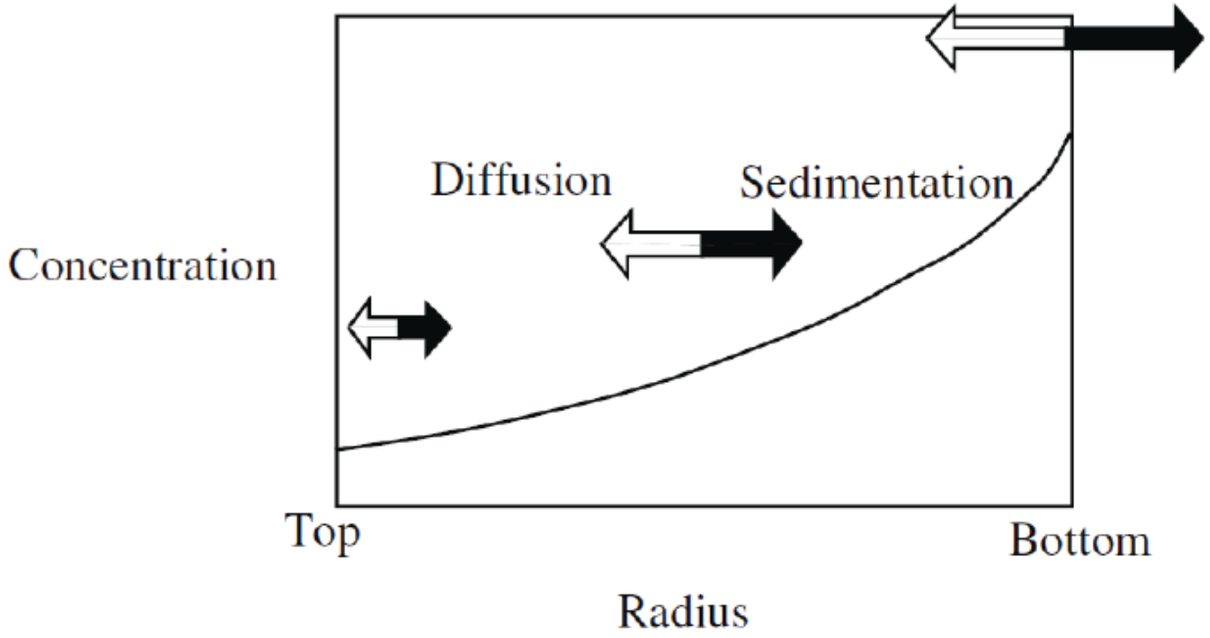

Figure 14. Schematic representation of sedimentation equilibrium. The flow of solute due to sedimentation (black arrows) increases with radial distance. This process is balanced at equilibrium by the reverse flow from diffusion (open arrows), which increases with concentration gradient. At equilibrium, the resulting concentration distribution is exponential with the square of the radial position.

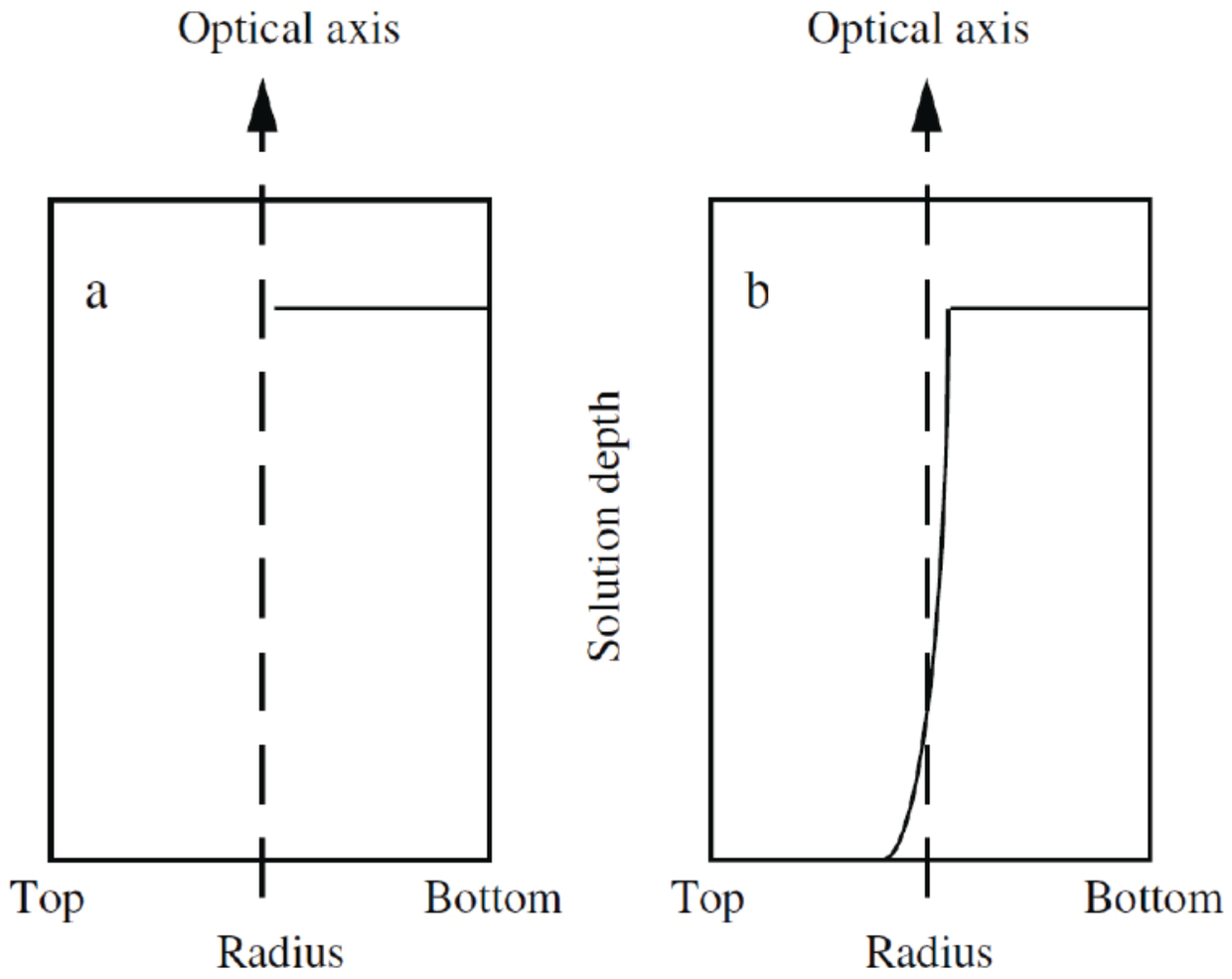

Figure 15. Schematic representation of the meniscus in a centrifuge cell. At high angular velocity (a) the meniscus is close to vertical and aligned with the optical axis. At low angular velocity (b) the meniscus is curved and is tilted with respect to the optical axis.

nanomaterials

MDPI

Review

Ultracentrifugation Techniques for the Ordering of Nanoparticles

The two important theoretical equations in the field of AUC are the Svedberg Equation and the Lamm Equation. In deriving the Svedberg equation, three forces are assumed to come into balance immediately in a centrifugal field, including sedimentation (F_s) and the counter acting buoyancy (F_b) and frictional (F_f) force which thus induce the sample species to move with a constant sedimentation velocity, as shown in Equation (1). With the expansion of these three forces and several rearrangements, the famous Svedberg Equation can be deduced, as shown in Equation (2) and its derivation for hard spheres in Equation (3) [68].

$$F_s + F_b + F_f = 0 \tag{1}$$

$$M = \frac{sRT}{D(1 - \bar{\nu}\rho_s)} \tag{2}$$

$$d_H = \sqrt{\frac{18\eta_s s}{(\rho_p - \rho_s)}} \tag{3}$$

where M is the molecular mass of the species, s is the sedimentation coefficient, R is the molar gas constant, T is the thermodynamic temperature, D is the diffusion coefficient, ρ_p and ρ_s are the density of the species and solvent respectively, $\bar{\nu}$ is the partial specific volume, d_H is the hydrodynamic diameter and η_s is the solvent viscosity.

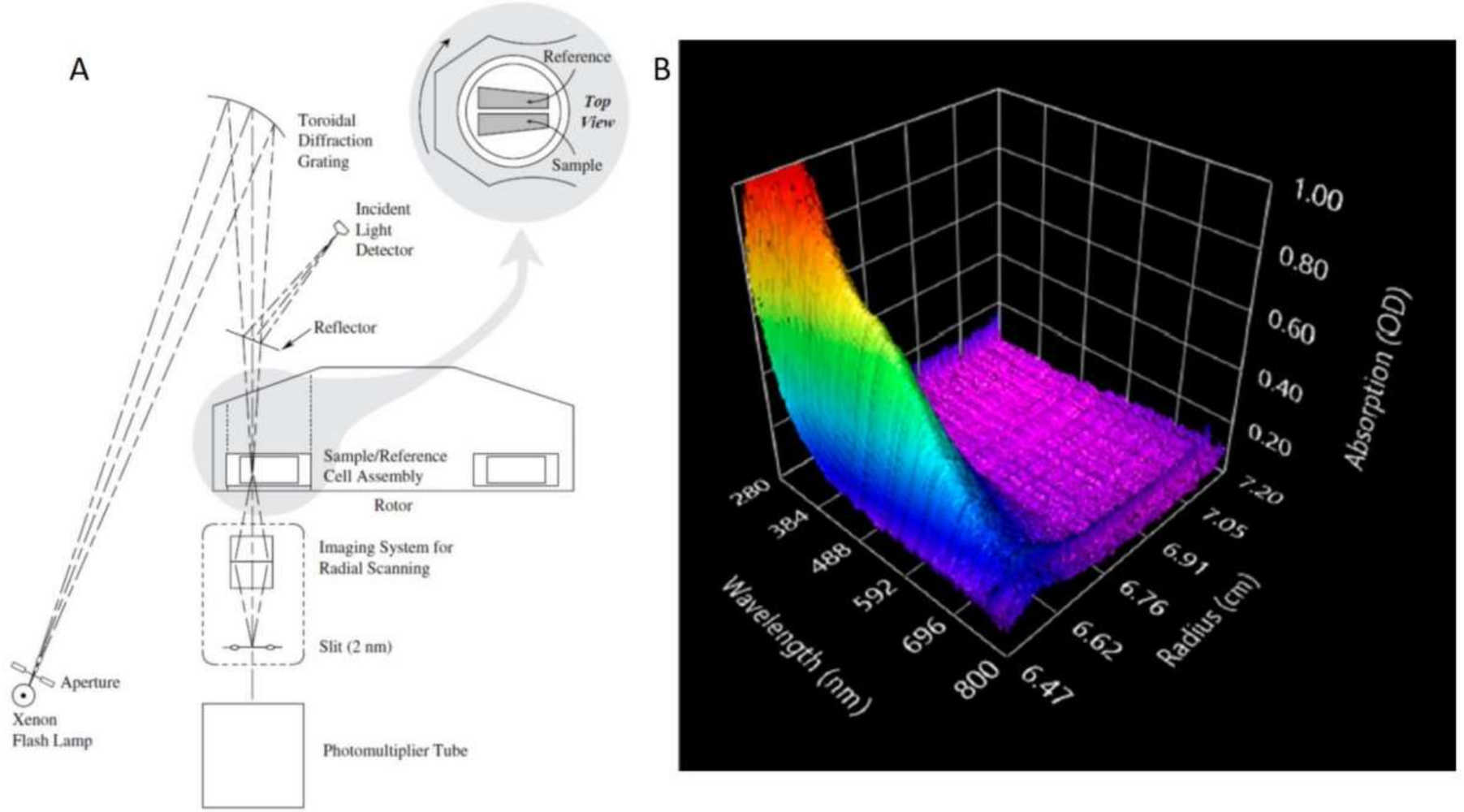

Figure 6. (**A**) Schematic setup of a Beckman CoulterTM Optima^{TM} XL-A Analytical UltraCentrifugation (AUC) instrument (with an UV absorption optic system). Reproduced with permission from [86], Copyright Beckman-Coulter, 1993. (**B**) Typical three-dimensional dataset result for an AUC experiment with a multi-wavelength (MWL) optical system.

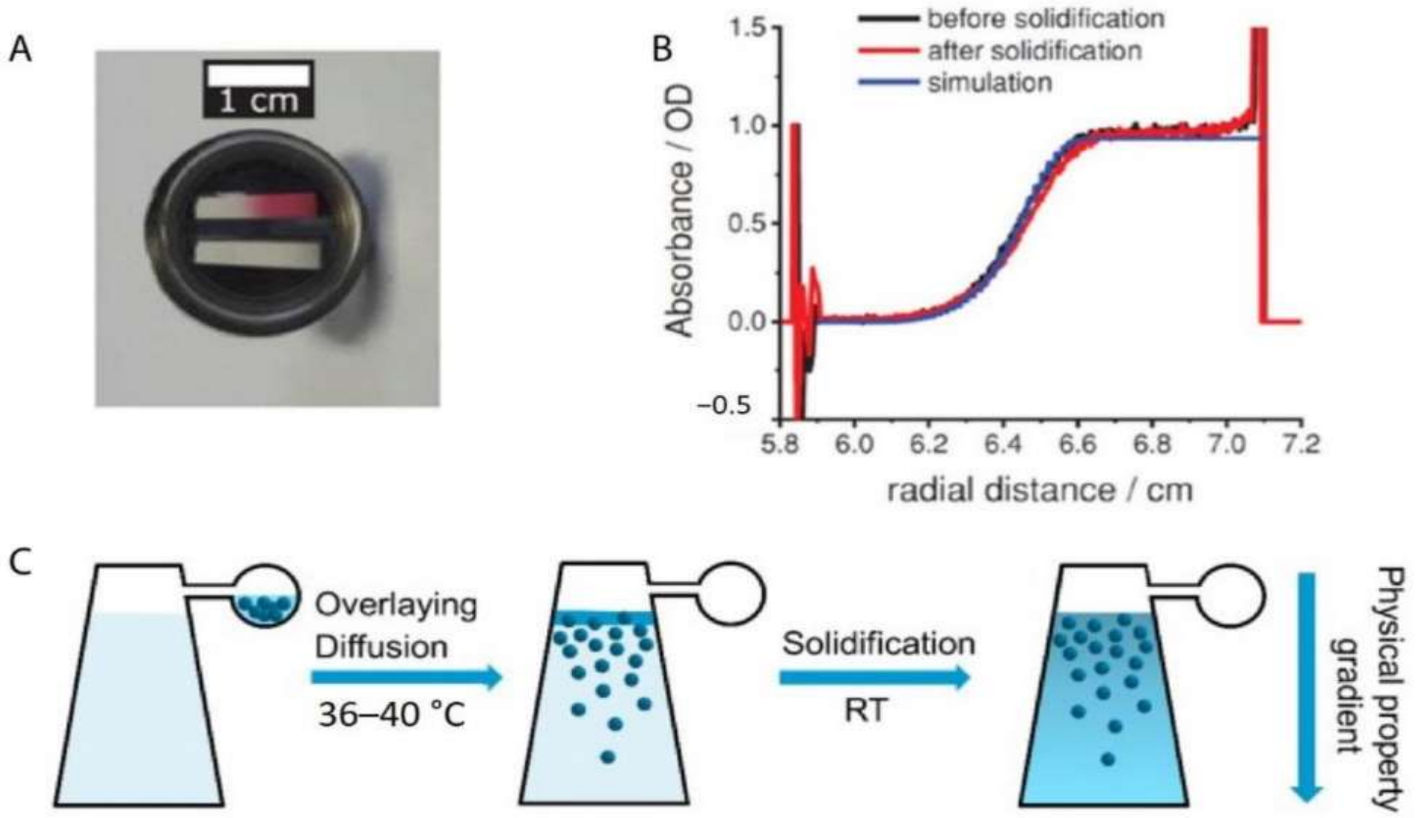

Figure 7. (**A**) Photograph of a piece of gradient nanoparticle superstructure made of spherical gold nanoparticles in gelatin inside an AUC centerpiece. The top sector is the sample sector with the nanoparticle gradient, while the bottom sector is the reference without any nanoparticles inside; (**B**) Absorbance profile of the gold nanoparticle concentration gradient, obtained after the centrifugation at 13,000 rpm for 32 min. The experimental gradient did not change after the solidification and agrees with the simulation results with the SEDFIT; (**C**) Schematic procedures to produce nanoparticle gradient superstructures in the sample sector of an analytical ultracentrifugation band-forming cell by the diffusion at a low angular velocity and subsequent solidification. Reproduced with permission from [98], Copyright Wiley-VCH, 2018.

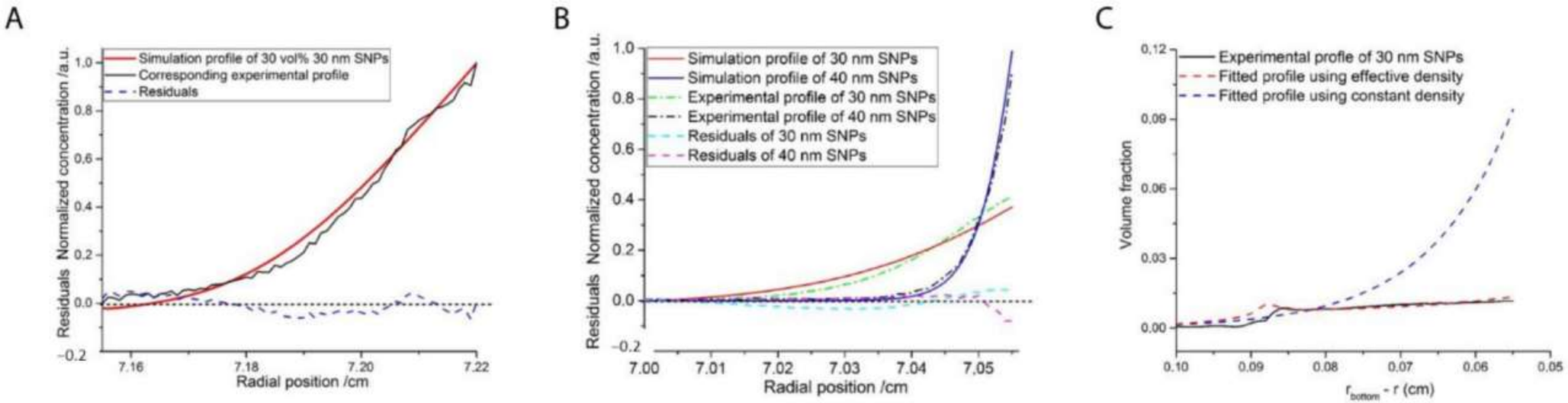

Figure 8. (**A**) Normalized experimental (black line) and simulation (red line) concentration (*c*) gradients for 30 nm hard-sphere-like silica nanoparticles of an initial concentration of 30 vol% in an AUC-SE experiment at 2800 rpm; the root-mean-square deviation (RMSD) value is 0.034% and the blue line corresponds to the deviation between experimental and simulation data; (**B**) Normalized experimental (dash dotted lines) and simulation (solid lines) concentration gradients for a binary hard sphere mixture of 30 nm (3.3 vol%) and 40 nm (6.7 vol%) silica nanoparticles in an AUC-SE experiment at 2800 rpm and the dashed line corresponds to the deviation between experimental and simulation data; (**C**) Experimental (solid line) and simulation (dashed lines) concentration gradients for 30 nm silica nanoparticles in a binary hard sphere mixture of 30 nm (1 vol%) and 90 nm (9 vol%) silica nanoparticles in an AUC-SE experiment at 2800 rpm, with the simulation profiles using the constant solvent density (blue dashed line) and the effective density (red dashed line); Reproduced with permission from [103], Copyright the American Chemical Society, 2019, and [106], Copyright Wiley-VCH, 2019.

A

B

C

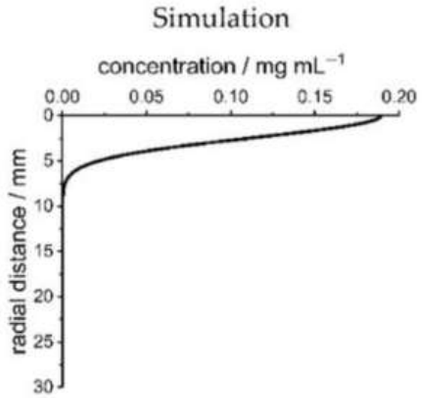
Simulation
concentration / mg mL⁻¹
0.00
0.05
0.10
0.15
0.20
radial distance / mm
0
5
10
15
20
25
30

D

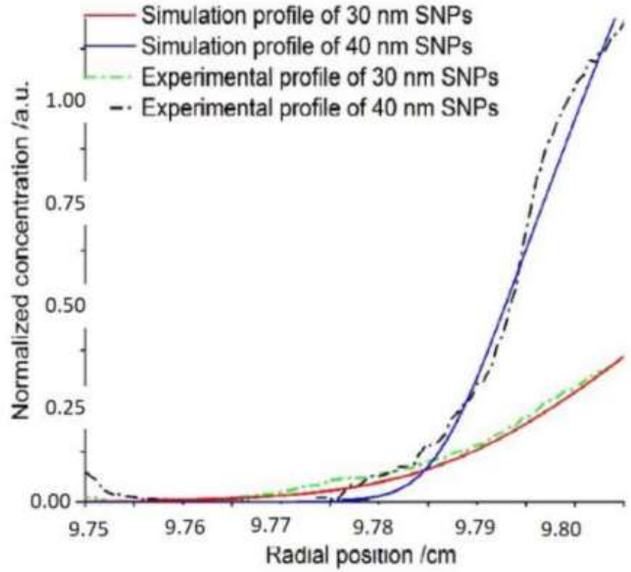
Simulation profile of 30 nm SNPs
Simulation profile of 40 nm SNPs
Experimental profile of 30 nm SNPs
Experimental profile of 40 nm SNPs
Normalized concentration /a.u.
1.00
0.75
0.50
0.25
0.00
9.75
9.76
9.77
9.78
9.79
9.80
Radial position /cm

Figure 9. (A) A typical piece of nanoparticle gradient material in a gelatin gel matrix made in an AUC cell from two different views with the dimension of 1.2 cm × 0.7 cm × 0.3 cm; (B) Typical piece of nanoparticle gradient material made in a cylindrical PUC tube with the length of 3.8 cm and diameter of 1.2 cm; (C) Piece of fluorescence labeled silica nanoparticle gradient material obtained after a PUC experiment at 3000 rpm for 20 h in a L-70 preparative ultracentrifuge with the corresponding simulated concentration gradient; (D) Normalized experimental (dashed dotted lines) and simulation (solid lines) concentration gradients for a binary hard sphere suspension of 30 nm (3.3 vol%) and 40 nm (6.7 vol%) silica nanoparticles with two different fluorescent labels from a PUC experiment at 2800 rpm in a L-70 preparative ultracentrifuge. The absorbance gradients were measured by a confocal laser scanning microscope (CLSM) and agreed with the simulations

Analytical Ultracentrifuge Analysis of Nucleosomes Assembled from Recombinant, Acid-Extracted, HPLC-Purified Histones

Manjinder S. Cheema and Juan Ausió

Abstract

The accumulating discoveries of new posttranslational modifications (PTMs) and the increasing relevance of histone variants within the frame of epigenetics demand the availability of methods for a rapid and efficient nucleosome reconstitution to analyze their structural and functional implications. Here we describe a method suitable for this purpose, starting from bacterially expressed histones, solubilized by acid and purified by reversed-phase high-performance liquid chromatography. This method allows the preparation of micrograms to milligram amounts of in vitro-assembled nucleosomes. Finally, we demonstrate the efficiency of this method for the structural analysis of nucleosomes in the analytical ultracentrifuge.

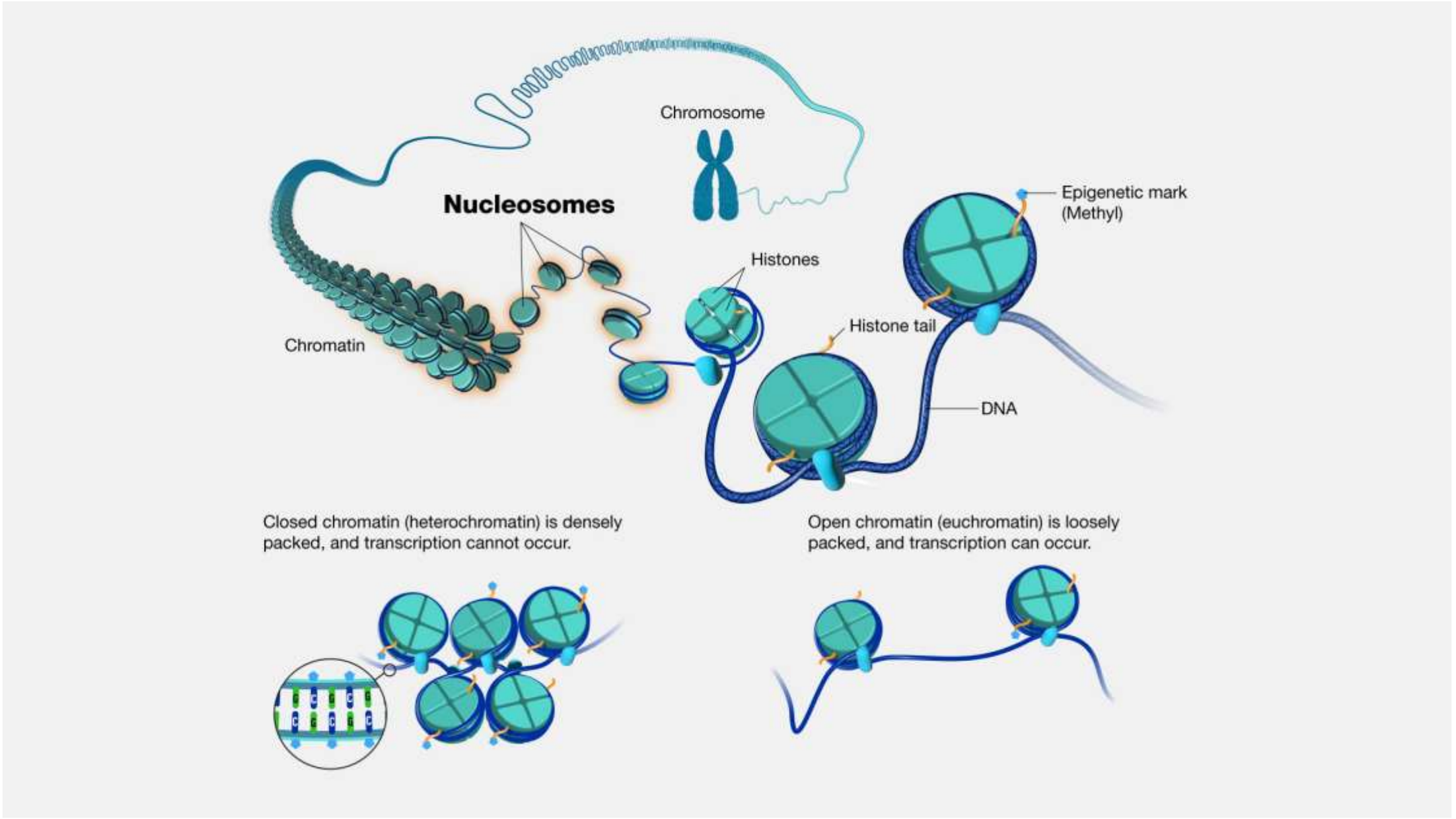
Chromosome
Nucleosomes
Chromatin
Histones
Histone tail
Epigenetic mark
(Methyl)
DNA
Closed chromatin (heterochromatin) is densely packed, and transcription cannot occur.
Open chromatin (euchromatin) is loosely packed, and transcription can occur.

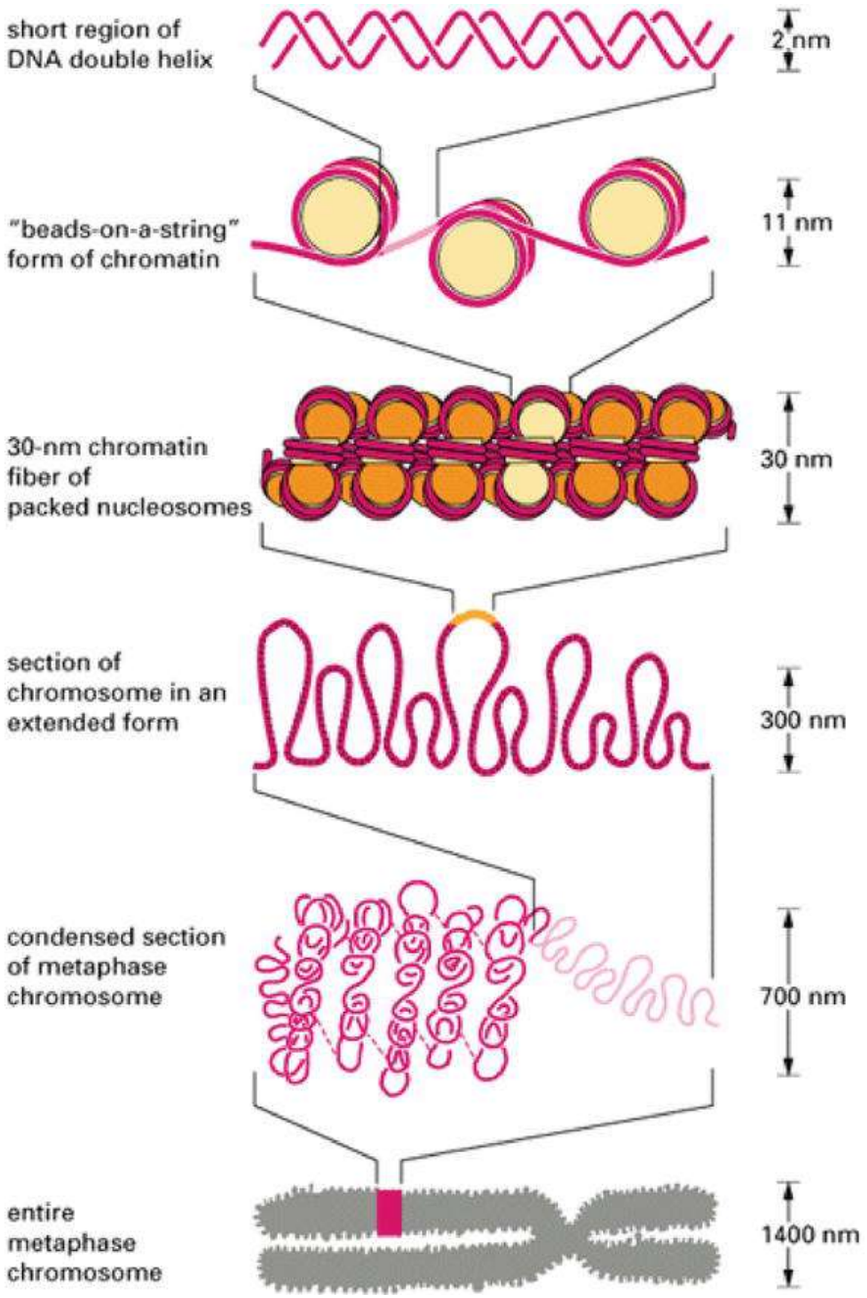
short region of
DNA double helix
2 nm
"beads-on-a-string"
form of chromatin
11 nm
30-nm chromatin
fiber of
packed nucleosomes
30 nm
section of
chromosome in an
extended form
300 nm
condensed section
of metaphase
chromosome
700 nm
entire
metaphase
chromosome
1400 nm

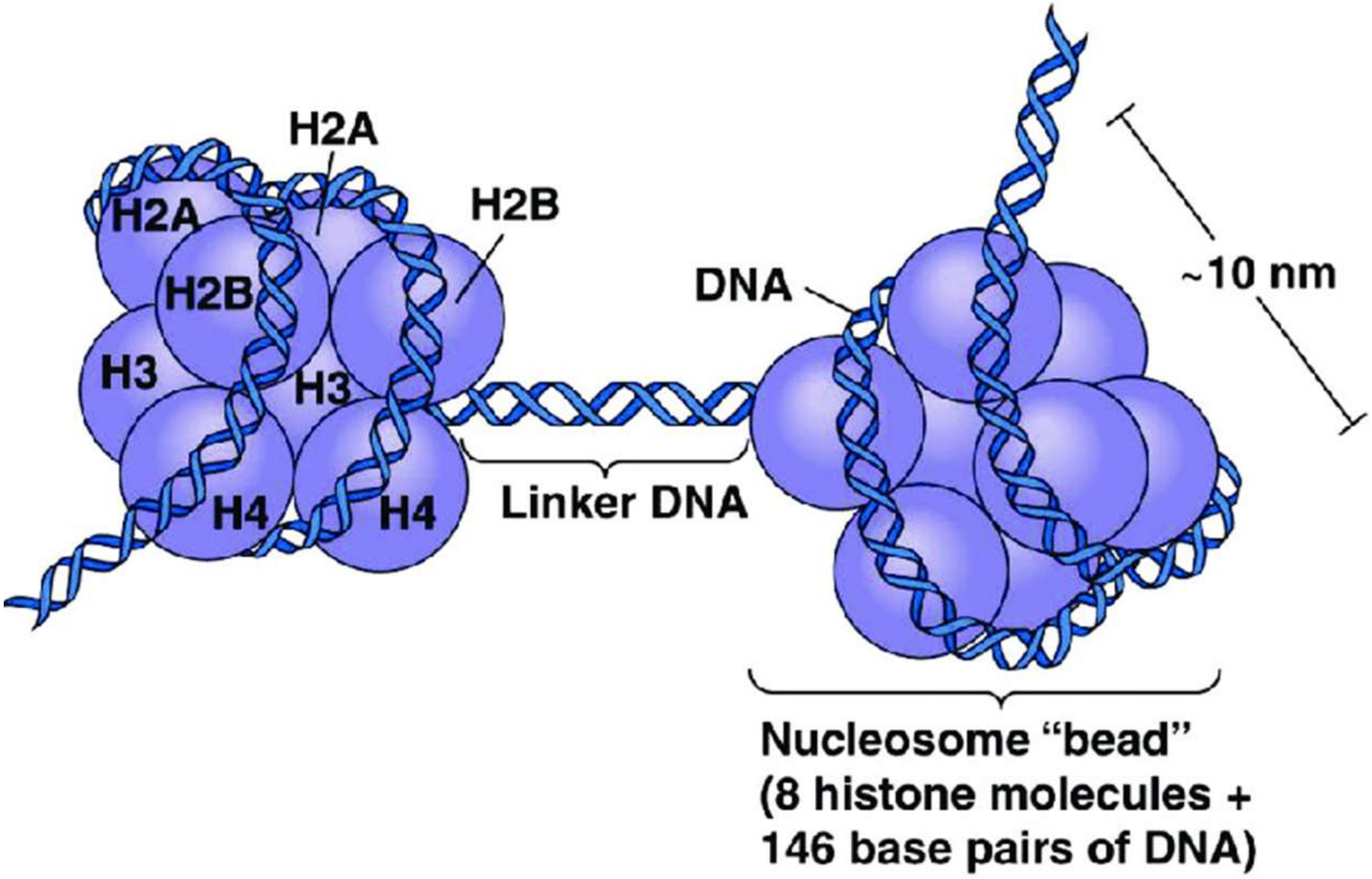
H2A
H2A
H2B
H2B
H3
H3
H4
H4
Linker DNA
DNA
~10 nm
Nucleosome "bead"
(8 histone molecules +
146 base pairs of DNA)

- A nucleosome is a section of DNA that is wrapped around a core of proteins.
- Inside the nucleus, DNA forms a complex with proteins called chromatin, which allows the DNA to be condensed into a smaller volume.
- When the chromatin is extended and viewed under a microscope, the structure resembles beads on a string.
- Each of these tiny beads is a called a nucleosome and has a diameter of approximately 11 nm.
- The nucleosome is the fundamental subunit of chromatin.
- Each nucleosome is composed of a little less than two turns of DNA wrapped around a set of eight proteins called histones, which are known as a histone octamer.
- **Each histone octamer is composed of two copies each of the histone proteins H2A, H2B, H3, and H4**.
- The chain of nucleosomes is then compacted further and forms a highly organized complex of DNA and protein called a chromosome.

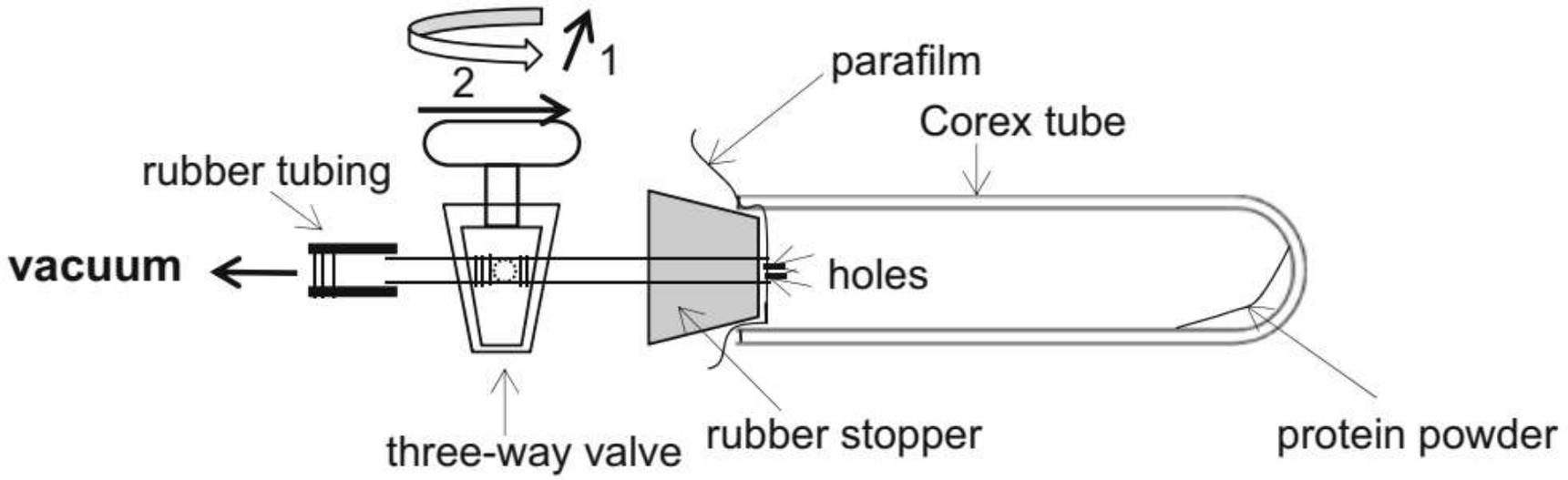

Fig. 1 To dry the protein pellets after precipitation of the acid-extracted proteins with acetone, a very simple device can be improvised from a glass three-way valve and a perforated rubber stopper connected to a vacuum source (vacuum pump or aspirator). The valve should be on its "closed" position (1) when the Corex centrifuge tube—with the precipitated protein pellet (*see* Subheading 3.1, **step 16**)—is attached to the rubber stopper, and in the "open" position (2) for drying. After the pellet is completely dry and powdery, the valve should be returned to position (1) before the centrifuge tube is gently detached

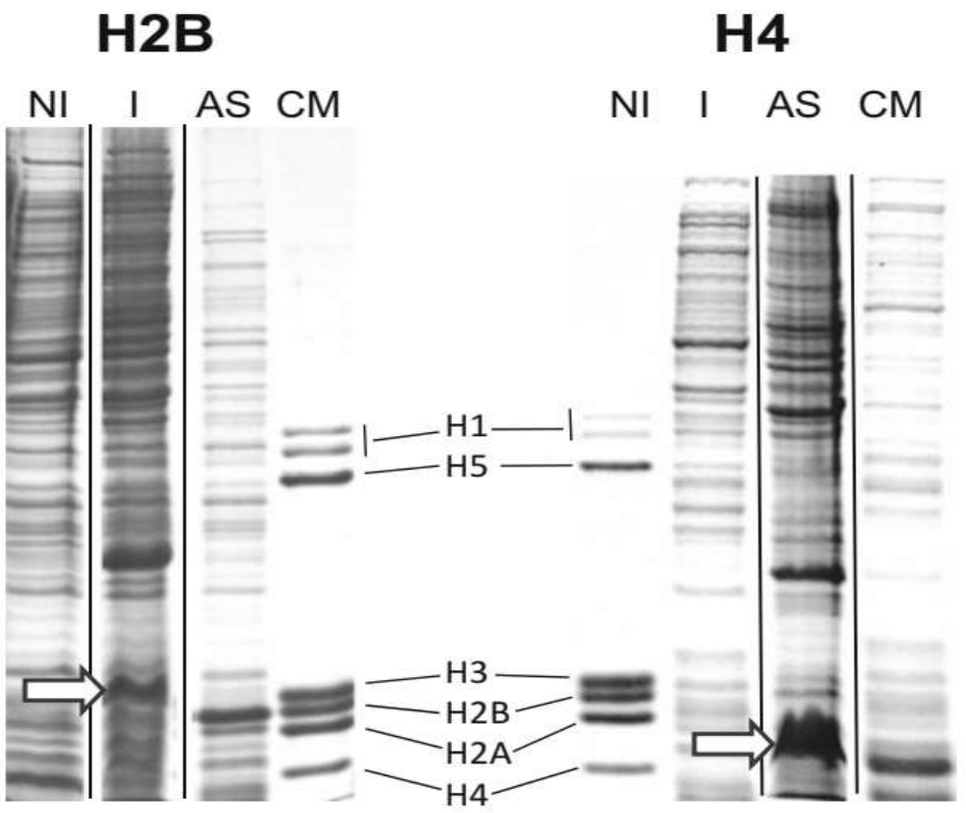

Fig. 2 SDS-PAGE analysis of the recombinant protein from bacteria expressing histone H2B and H4, before IPTG induction (NI), after IPTG induction (I), and after 0.5 N HCl solubilization (*see* Subheading 3.1) (AS). The *arrow* indicates the histone expressed. The slight decrease in its electrophoretic mobility compared to the marker is due to the composition of sample buffer used to solubilize the bacterial pellet. *CM* chicken erythrocyte histone marker. The *vertical lines* are there to indicate that the images were taken from different noncontiguous regions of the same gel

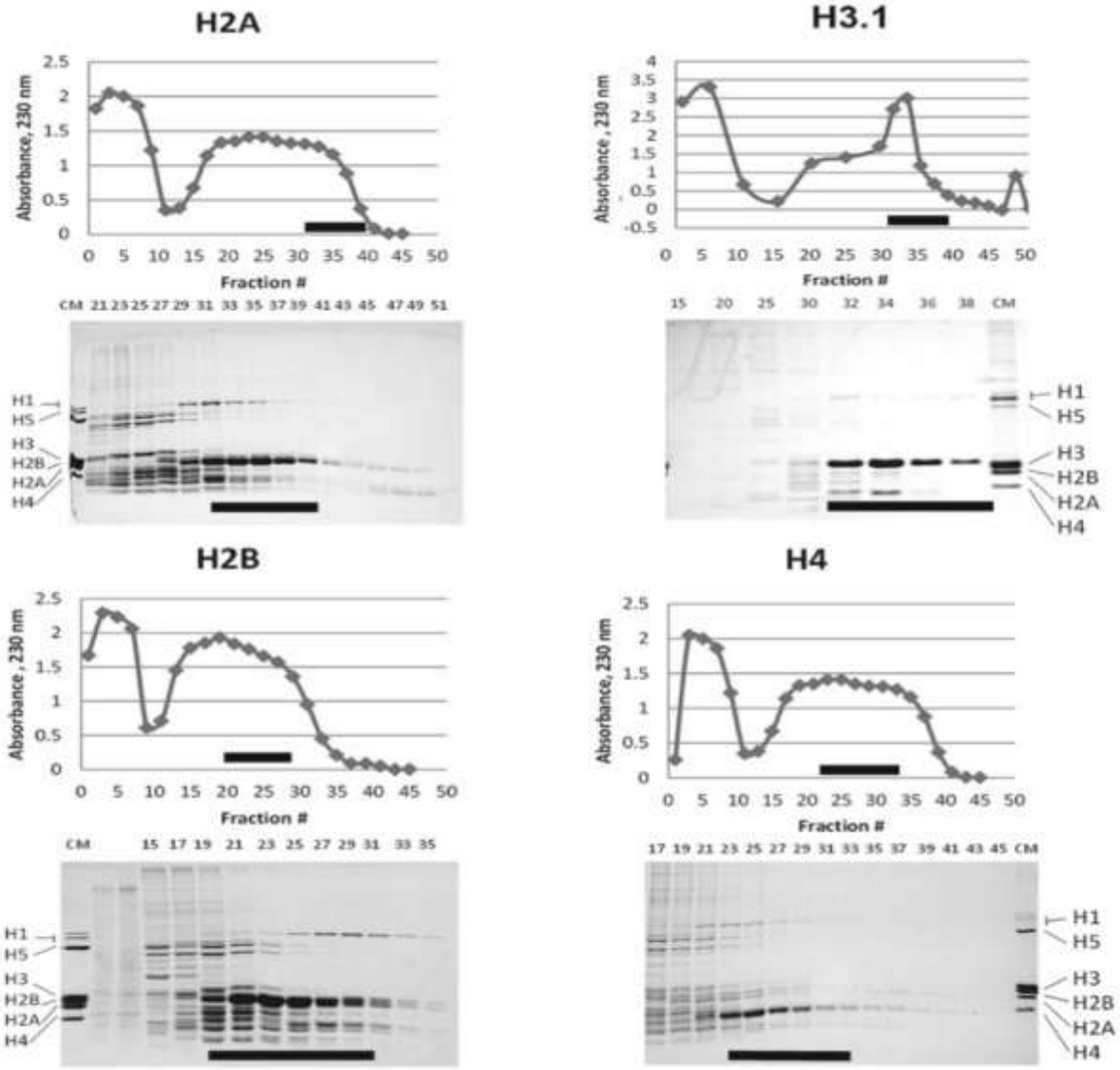

Fig. 3 Ionic exchange fractionation (*see* Subheading 3.2, **step 17**) and SDS-PAGE analysis of the acid-soluble fractions (*see* Subheading 3.1, **step 19**). The fraction numbers are indicated on *top* of the gel. The *bars* indicate the fractions pooled. Elution conditions are as described in the text. *CM* chicken erythrocyte histone marker

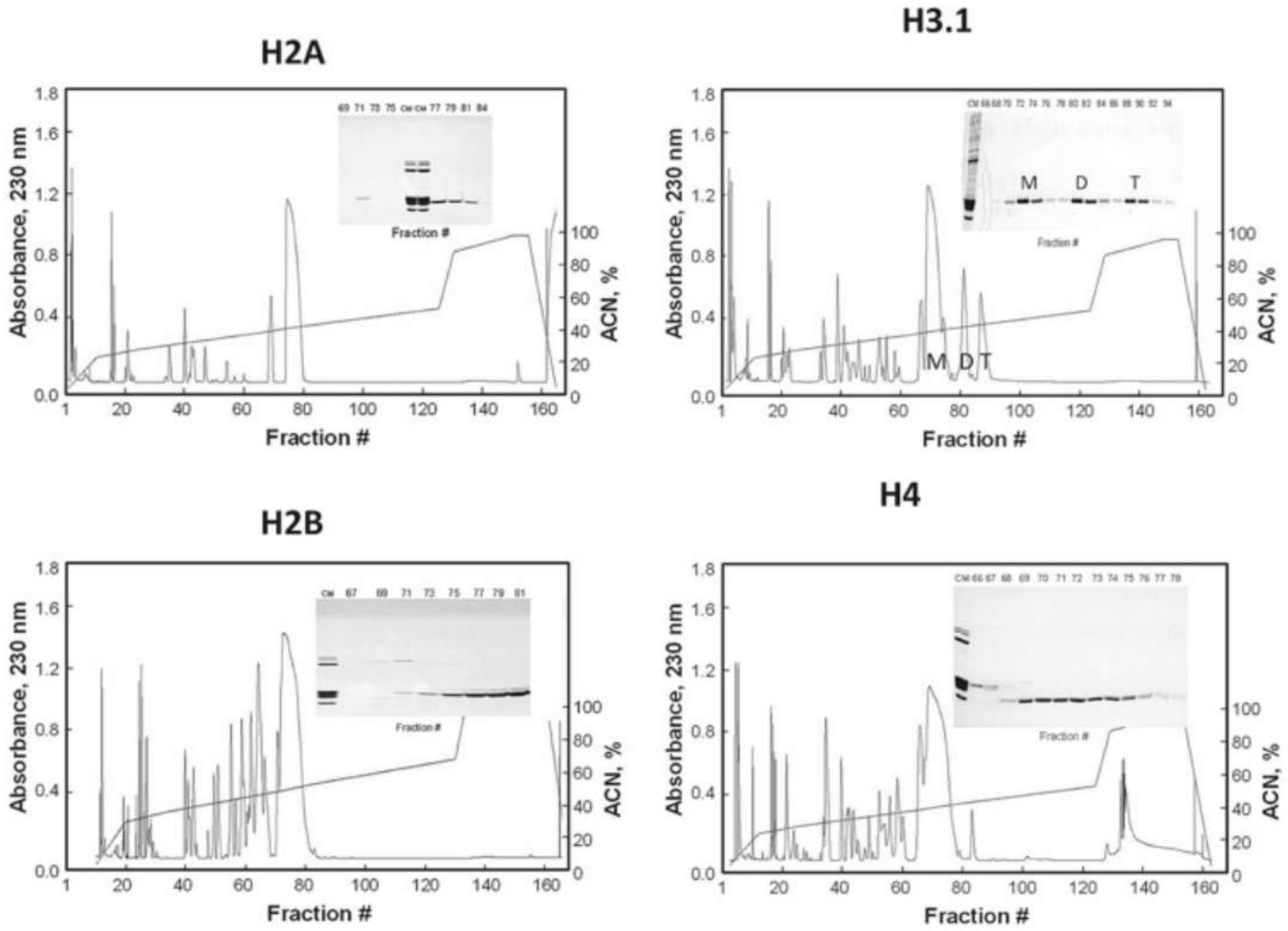

Fig. 4 Reversed-phase HPLC fractionation and SDS-PAGE analysis (*inset*) of the fractions pooled in Fig. 3. T fraction numbers are indicated on *top* of the gel. The elution conditions are indicated in the text (*s* Subheading 3.3, **step 3**). *CM* chicken erythrocyte histone marker

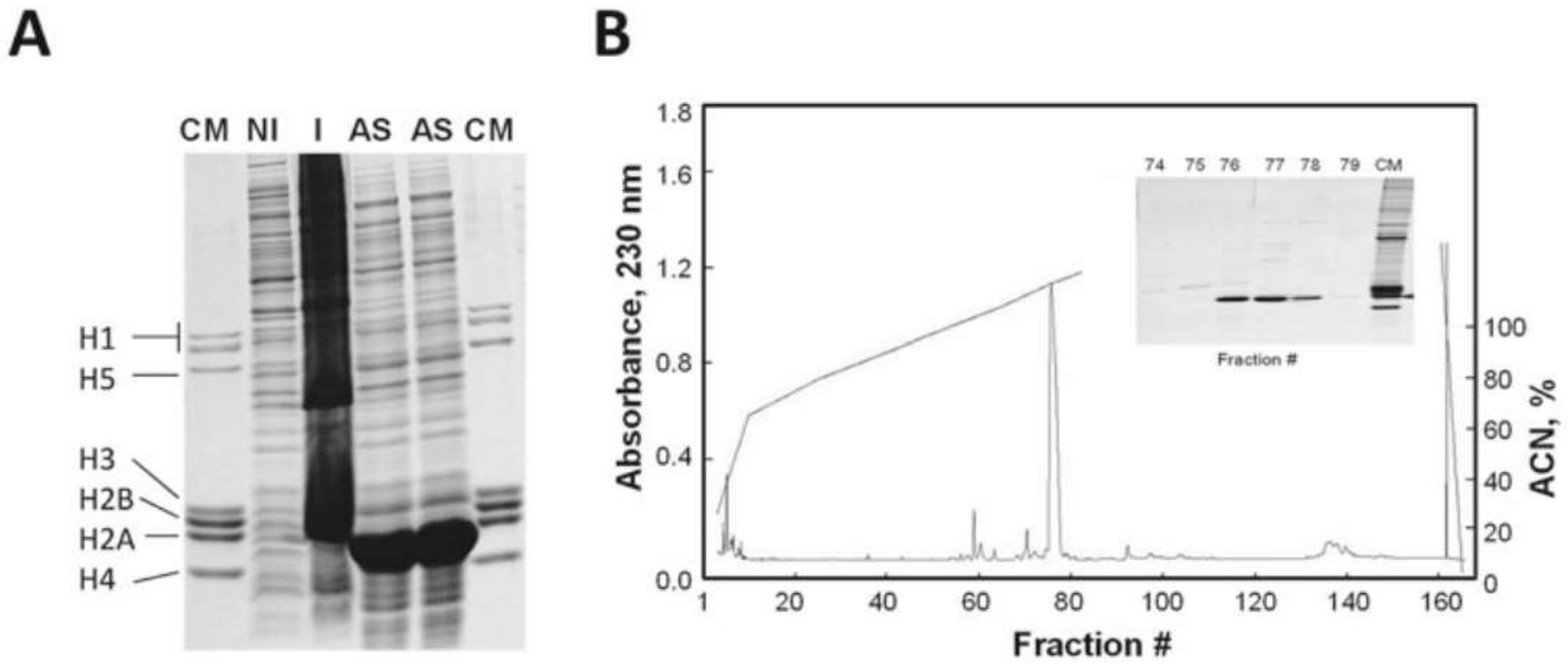

Fig. 5 (**a**) SDS-PAGE analysis of a bacterial culture expressing histone H2A.Z-1, grown for 3 h at 37 °C after induction with IPTG at an $OD_{600} = 0.6$. *NI* protein sample before induction, *I* protein sample after induction, *AS* 0.5 N HCl acid-soluble fraction (*see* Subheading 3.1) (**b**). Reversed-phase HPLC of the sample shown in (**a**) lane AS. *CM* chicken erythrocyte histone marker. The *inset* shows an SDS-PAGE analysis of some of the fractions collected during the elution

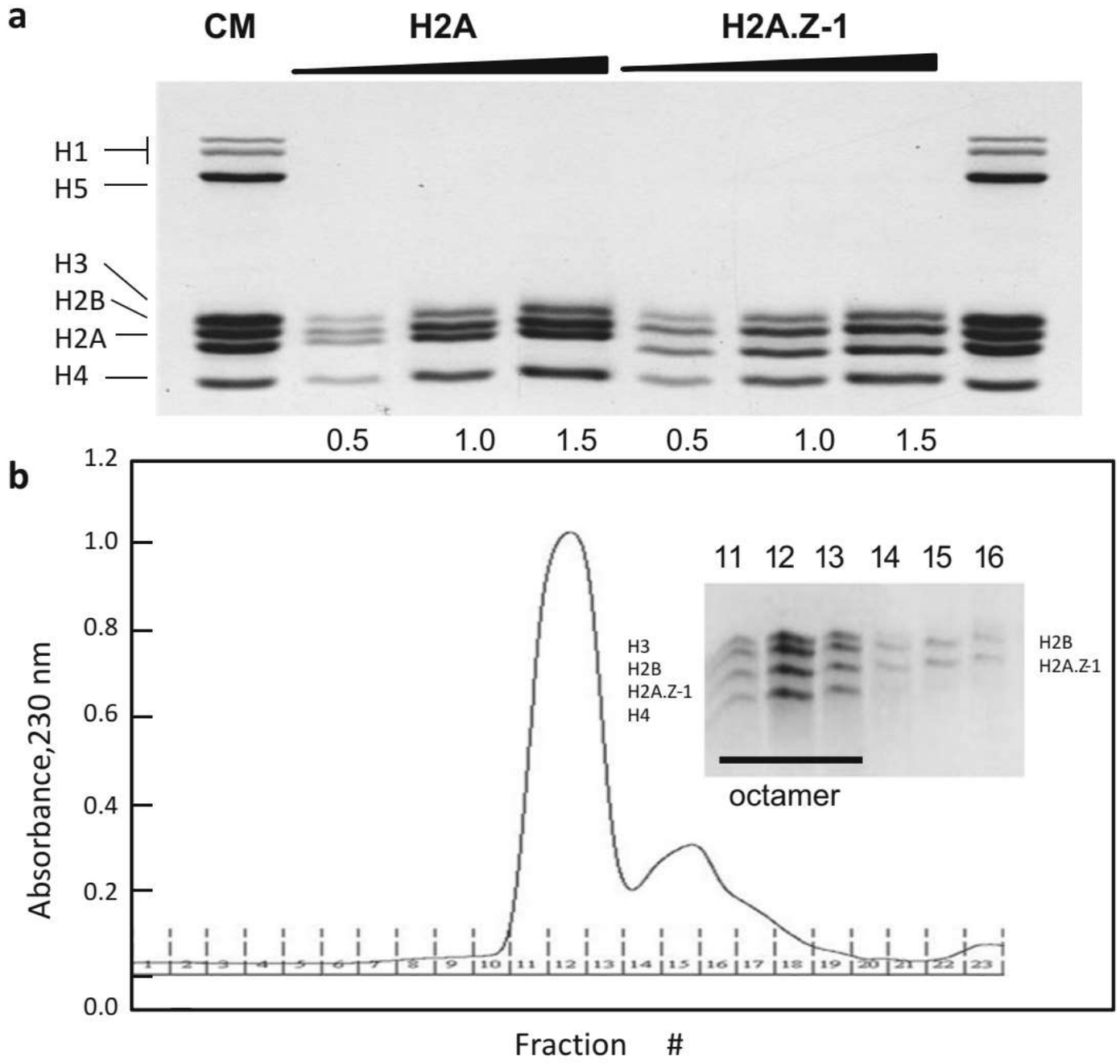
a
CM
H2A
H2A.Z-1
H1
H5
H3
H2B
H2A
H4
0.5
1.0
1.5
0.5
1.0
1.5
b
Absorbance,230 nm
1.2
1.0
0.8
0.6
0.4
0.2
0.0
11 12 13 14 15 16
H3
H2B
H2A.Z-1
H4
H2B
H2A.Z-1
octamer
Fraction #

Fig. 6 (a) Increasing amount of purified histone mixtures dissolved in water, consisting of approximately equal amounts of each individual histone as estimated from the concentration determined of their absorbance at 230 nm. (H3-H4-H2B)-H2A and (H3-H4-H2B)- H2A.Z-1 mixtures are shown. The numbers below indicate the approximate number of micrograms loaded in each lane.

(b) FPLC chromatogram of an (H3-H4-H2B)-H2A.Z-1 mixture after octamers. The inset shows an SDS-PAGE analysis of some of the fractions collected along the elution profile. The bar indicates the fractions corresponding to the histone octamer.

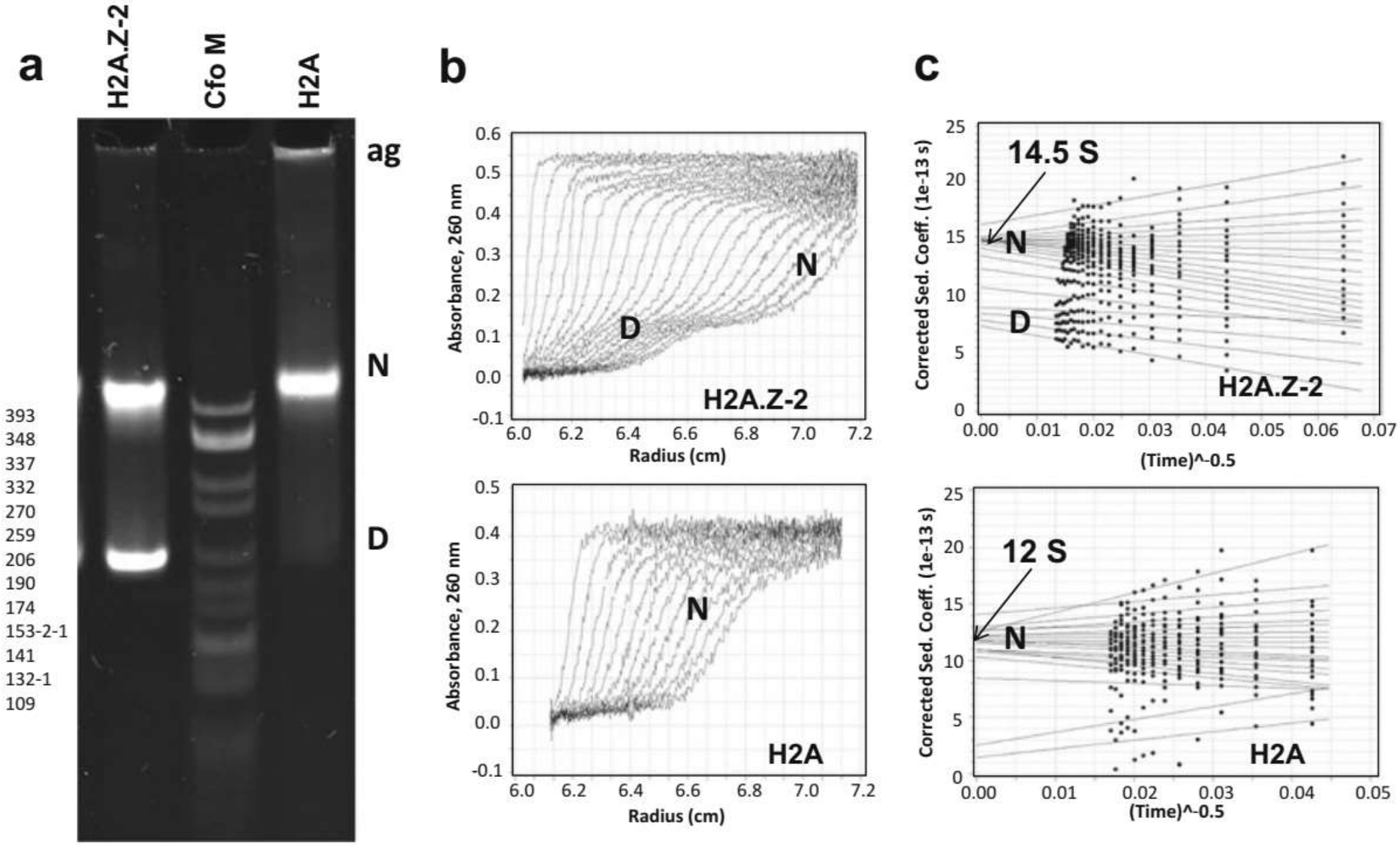
a
H2A.Z-2
Cfo M
H2A
ag
N
D
393
348
337
332
270
259
206
190
174
153-2-1
141
132-1
109
b
Absorbance, 260 nm
Radius (cm)
N
D
H2A.Z-2
H2A
c
Corrected Sed. Coeff. (1e-13 s)
(Time)^-0.5
14.5 S
12 S
N
D
H2A.Z-2
H2A

Fig. 7 (a) Ethidium bromide-stained native 4 % PAGE of nucleosomes consisting of (H3-H4-H2B)-H2A (lane H2A) and (H3-H4-H2B)-H2A.Z-2 (lane H2A.Z-2), reconstituted onto a 208 bp DNA template. Notice the downward shift in electrophoretic of the (H3-H4-H2B)-H2A.Z-2-containing nucleosome. ag aggregates, D = 208 bp DNA; Nucleosome, Cfo M pBr322 plasmid DNA digested with CfoI, used as a marker. The number of bp corresponding to the bands is indicated on the left. The amount of free DNA in the H2A.Z-2 nucleosomes (approx. 15 %, see Fig. (b)—H2A.Z-2) does not reflect any difference in its reconstitution efficiency compared to the H2A nucleosome, but simply indicates a lower amount of histones loaded at the start of the reconstitution. Notice that the brightest appearance of the DNA band (D) is due to the fact that free DNA is able to intercalate three times more ethidium bromide than when reconstituted into nucleosomes (N). (b) Sedimentation profiles of the H2A and H2A.Z-2 nucleosome samples in the AUC. (c) Analysis of the boundaries shown in (b) using the “ fan plot” representation of the van Holde and Weischet] analysis method. In this representation, the number of lines converging to a point in the “y-axis” is proportional to the amount of sample sedimenting, with its corresponding sedimentation coeffi cient indicated on this axis. Notice that the higher average sedimentation coefficient value of the H2A.Z-2 nucleosomes (14.5 S) indicates a more compact conformation when compared to the H2A nucleosome (12 S), in agreement with the change in electrophoretic mobility observed in (a)

THANK YOU